

Modelling of image formation and registration at photographic materials

T.V.Danilova

Saratov State Technical University, Saratov, Russia

ABSTRACT

In this paper we present the model of photographic image formation and the light leakage at emulsion layers of photographic materials. Result of modelling is spatial distribution of exposed silver grains at photographic emulsion layers. We found the influence of some photographic material parameters to image characteristics. Distribution of optical density for real images and results of modeling are also presented.

1. INTRODUCTION

Photographic materials are light sensitive materials that produce images as a response to the light energy incident upon it. This sensitivity is based on the chemical interaction of silver halide with light energy to produce metallic silver. Photographic materials consist of microscopic silver halide grains embedded in a gelatin (photographic emulsion). The mean grain diameter is 1.0 μm for ordinary emulsions. For special photographic materials range the mean grain sizes is greater. In this work, we consider emulsion with grain diameters are 0.5-2.5 μm , distribution of the grains sizes is normal. Volume of silver halide is 0.11 from total quantity of photographic emulsion. When exposed to light, these grains undergo a chemical change to form an invisible latent image. In consequence the development process latent image becomes realized. The set of metallic silver grains gives the photographic material its visible density^{1,2}.

Internal scattering between the grains within an emulsion causes a degradation of the recorded image. In this paper the process of photographic image formation and the light leakage at photographic emulsion layers are described by simple physical model.

2. PHYSICAL MODEL

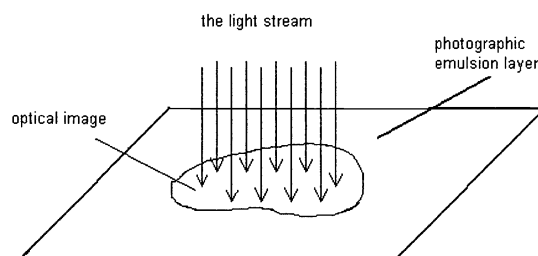


Fig. 1. Photographical emulsion layer exposure by light stream

The light focused by optical system at the surface of photographic emulsion layer (Fig. 1)³. The wavelength of light is known.

$$\Phi(r, t) = A \exp(-i(\omega t - kr)) \quad (1)$$

If the vector of light stream is parallel with OZ, then the electric and magnetic components of light stream can be expressed as

$$\begin{aligned}
E_x &= \exp(ikz) & E_y &= 0 & E_z &= 0 \\
H_x &= 0 & H_y &= \frac{ik}{k_2} \exp(ikz) & H_z &= 0
\end{aligned} \tag{2}$$

$$k_1 = \frac{i\omega}{c} \left(\varepsilon + i \frac{4\pi\sigma}{\omega} \right) \quad k_2 = \frac{i\omega}{c} \quad k^2 = -k_1 k_2$$

Density of light stream energy described by expression:

$$S = c\varepsilon E^2 \tag{3}$$

Let's light stream is collinear and normal to surface of photographic emulsion layer. The mean size and size distribution of grains are known. Space distribution of grain is even.

In this work we model the process of photographic image formation and the light leakage at photographic emulsion layers. The input data for this model are height, width, thickness of photographic emulsion layer, volume of silver halide, size and shape of exposed area.

Result of modeling is spatial distribution of exposed silver grains at photographic emulsion layers.

3. NUMERICAL MODEL

3.1 Modelling of the light leakage at photographic emulsion layers

The form of photographic emulsion grains are modeling by the ball, therefore we will use spherical coordinate system. In this case, the EH-field components (2) are

$$\begin{aligned}
E_r &= \exp(ikr \cos \theta) \sin \theta \cos \varphi, \\
E_\theta &= \exp(ikr \cos \theta) \cos \theta \cos \varphi, \\
E_z &= -\exp(ikr \cos \theta) \sin \varphi, \\
H_r &= \frac{ik}{k_2} \exp(ikr \cos \theta) \sin \theta \sin \varphi, \\
H_\theta &= \frac{ik}{k_2} \exp(ikr \cos \theta) \cos \theta \sin \varphi, \\
H_\varphi &= \frac{ik}{k_2} \exp(ikr \cos \theta) \cos \varphi \tag{3}
\end{aligned} \tag{4}$$

The wavelength is comparable to mean size of grains, for E and H component calculations the Mie Theory was applied. Let's assume centre of grain coincide with centre of coordinate. According to Mie Theory stray field from isolated grain may be described as:

$$\begin{aligned}
E_r^{(s)} &= \frac{1}{(k^{(1)})^2} \frac{\cos \varphi}{r^2} \sum_{l=1}^{\infty} l(l+1)^\varepsilon B_l \xi_l^{(1)'}(k^{(1)}r) \pi_l \sin \theta \\
E_\theta^{(s)} &= \frac{1}{k^{(1)}} \frac{\cos \varphi}{r} \sum_{l=1}^{\infty} \left\{ {}^e B_l \xi_l^{(1)'}(k^{(1)}r) \tau_l + i^m B_l \xi_l^{(1)}(k^{(1)}r) \pi_l \right\}, \\
E_\varphi^{(s)} &= -\frac{1}{k^{(1)}} \frac{\sin \varphi}{r} \sum_{l=1}^{\infty} \left\{ {}^e B_l \xi_l^{(1)'}(k^{(1)}r) \pi_l + i^m B_l \xi_l^{(1)}(k^{(1)}r) \tau_l \right\}, \\
H_r^{(s)} &= \frac{i}{k^{(1)} k_2^{(1)}} \frac{\sin \varphi}{r^2} \sum_{l=1}^{\infty} l(l+1)^m B_l \xi_l^{(1)}(k^{(1)}r) \pi_l \sin \theta,
\end{aligned} \tag{5}$$

$$H_{\theta}^{(s)} = -\frac{1}{k^{(1)}} \frac{\sin \varphi}{r} \sum_{l=1}^{\infty} \left\{ {}^e B_l \xi_l^{(1)}(k^{(1)}r) \pi_l - i {}^m B_l \xi_l^{(1)}(k^{(1)}r) \tau_l \right\},$$

$$H_{\varphi}^{(s)} = \frac{1}{k_2^{(1)}} \frac{\cos \varphi}{r} \sum_{l=1}^{\infty} \left\{ i {}^m B_l \xi_l^{(1)}(k^{(1)}r) \pi_l - {}^e B_l \xi_l^{(1)}(k^{(1)}r) \tau_l \right\},$$

where

$${}^e B_l = i^{l+1} \frac{2l+1}{l(l+1)} \frac{n \psi_l'(q) \psi_l(nq) - \psi_l(q) \psi_l'(nq)}{\hat{n} \xi_l^{(1)}(q) \psi_l(\hat{n}q) - \xi_l^{(1)}(q) \psi_l(\hat{n}q)}, \quad (6)$$

$${}^m B_l = i^{l+1} \frac{2l+1}{l(l+1)} \frac{\hat{n} \psi_l(q) \psi_l'(\hat{n}q) - \psi_l'(q) \psi_l(\hat{n}q)}{\hat{n} \xi_l^{(1)}(q) \psi_l(\hat{n}q) - \xi_l^{(1)}(q) \psi_l(\hat{n}q)},$$

$$\pi_l = \frac{P_l^1}{\sin \theta} \quad \tau_l = \frac{dP_l^1}{d\theta} \quad \xi_l(\rho) = \sqrt{\frac{\pi \rho}{2}} H_{l+\frac{1}{2}}^{(1)} = \rho h_l^{(1)}(\rho) \quad \psi_l(\rho) = \sqrt{\frac{\pi \rho}{2}} J_{l+\frac{1}{2}}(\rho) = \rho j_l(\rho) \quad (7)$$

and wave numbers:

$$k_1^{(I)} = i \frac{2\pi}{\lambda_0} \varepsilon^{(I)} \quad k_2^{(I)} = i \frac{2\pi}{\lambda_0} \quad k^{(I)} = \frac{2\pi}{\lambda_0} \quad (8)$$

$$k_1^{(II)} = i \frac{2\pi}{\lambda_0} \left(\varepsilon^{(II)} + i \frac{4\pi\sigma}{\omega} \right) \quad k_2^{(II)} = i \frac{2\pi}{\lambda_0} \quad k^{(II)} = \frac{2\pi}{\lambda_0} \sqrt{\varepsilon^{(II)} + i \frac{4\pi\sigma}{\omega}}$$

$$q = \frac{2\pi}{\lambda^{(I)}} a \quad \hat{n} = \frac{k^{(II)} k_2^{(I)}}{k^{(I)} k_2^{(II)}} \quad (9)$$

a – diameter of the grain, $h_l^{(1)}$ – Hankel functions, j_l – spherical Bessel functions; P_l^1 – Legendr polynomials.

All functions calculated by recurrent scheme. Legendr polynomials and Hankel functions was calculated by using of the recursive methods. When the number series values is more then nearest integer of $q + 4q^{1/3} + 2$, the calculations are stopped^{4,5}.

3.2 Image acquisition at visualization plane

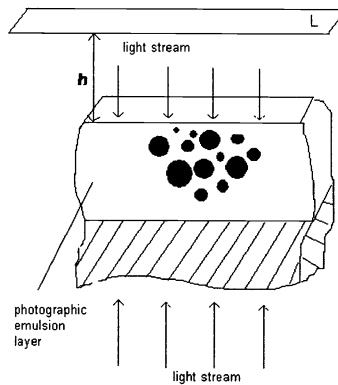


Fig. 2. Image acquisition at visualization plane. L – visualization plane, h – distance between photographic emulsion layer and visualization plane.

For estimation of optical density distribution let's consider system, that consist of exposed photographic emulsion layer that parallel with visualization plane (the plane where the some photosensor (human eye, videosensor, light sensitive element of scanning device etc.) can be placed (Fig. 2)). Light stream pass throw emulsion layer and make image at visualization plane. The optical density of each point for image at visualization plane is proportional to sum of stray fields of all exposed grains in this point.

4. SIMULATION

4.1 Stray field diagram for single grain

We calculate stray fields of single grain for different values of wavelength light, mean grain sizes. The Fig. 3 present stray field diagram for single grain.

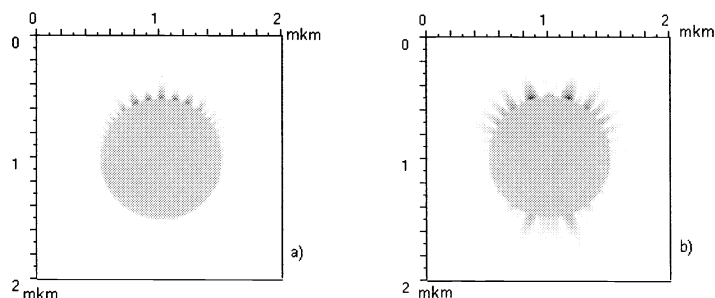


Fig. 3. Stray field diagram of single grain. Grain diameter is 1.0 mkm. Wavelength is a) 0.340 mkm, b) 0.500 mkm.

4.2 Light leakage at photographic emulsion layers

The process of light scattering by photographic emulsion layers was modeled (Fig. 4). The height and width of all layers are 20 mkm. The exposed area is 6-14 mkm. Wavelength of light is 0.350 mkm for (a), (c), (e) and 500 mkm for (b), (d), (f). Mean grain diameter is 0.500 mkm for (a), (b), 1.100 mkm for (c), (d), 2.200 mkm for (e), (f).

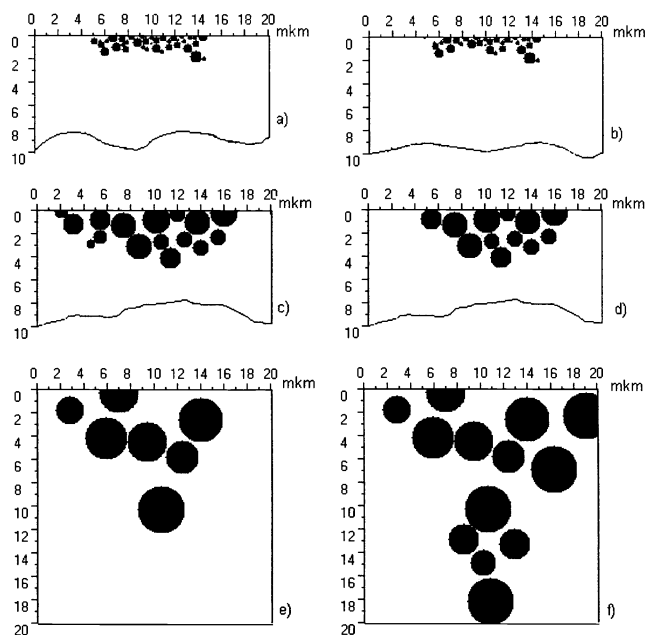


Fig. 4. Spatial exposed grains distributions

As is seen from modelling results the scattering light features is depends upon the light wavelength and size of photographic emulsion grains. Large-grained emulsions are more photosensitive. Large-grained emulsions are more scattering for red light. Fine-grained emulsions are more scattering for blue light. These conclusions are concerned with experimental results^{2,3}.

4.3 The optical density distribution of the model and the test object

For comparison the result of modelling with experiment dates the simple was used. The objects (fragment of electron microscopy grid) has rectangle shape and width of this objects is 10.0 mkm. . Photographic image for the test object was fabricated by contacting method. We estimate the optical density for this object and it's photographic image.

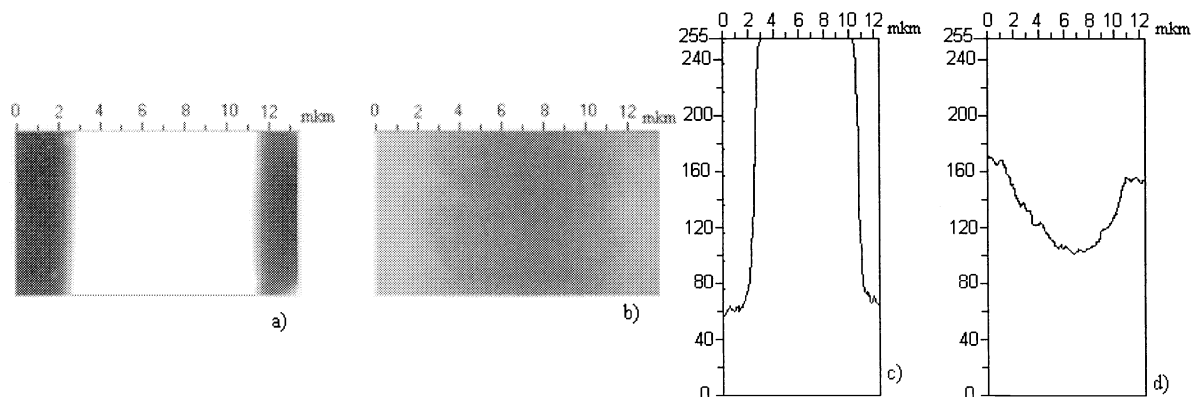


Fig. 5. Test object, photographic image of the test object and distributions of optical density for each.

The Fig. 5 present the test object, the photographic image of the test object, the distribution of optical density for the test object and distribution of optical density for the photographic image of this object. We created the model of the test object photographic image and calculated the optical density distribution for this model. The optical density distribution of model is estimated for different distances between photographic emulsion layer and visualization plane. The optical density distributions are presented at Fig. 6.

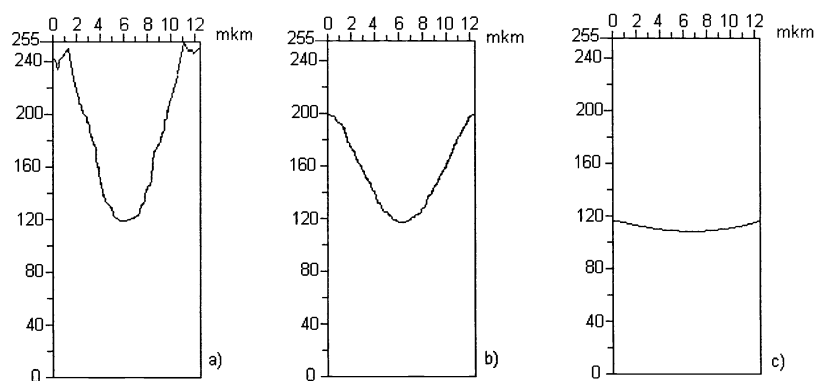


Fig. 6. Optical density distribution of model for distance between photographic emulsion layer and visualization plane is a) 1.0 mkm, b) 10.0 mkm, c) 100.0 mkm.

As is seen from Fig 6, when distance between visualization plane and photographic emulsion layer is enlarged, image is blur and become imperceptible.

Thus, we developed the model of photographic image formation which enough comparable to results of experiment dates.

5. SUMMARY

We generated the model of photographic image formation and the light leakage at photographic emulsion layers. Spatial distribution of exposed silver grains at photographic emulsion layers was calculated by this model. The results of modelling are used for estimate of images degradation. The optical density distributions for the test object and his model are presented.

REFERENCES

1. Mason L. F. A. Photographic Processing Chemistry. The Focal Press. London and New York, 1965, 208-209.
2. Altman J.H. The Sensitometry of Black and White Materials, ed., The Theory of the Photographic Process. 4^b Edition, Macmillian 1977.
3. Kingslake R. Optics in Photography, SPIE Optical Engineering Press, Bellingham, WA, 1992.
4. Kerker M. The Scattering of Light and Other Electromagnetic Radiation. Academic, New York, 1969.
5. Faxvog F.R., Roessler D.M. "Optical Absorption in Thin Slabs and Spherical Particles." *Appl. Opt.* **20**, 729-731 (1981).